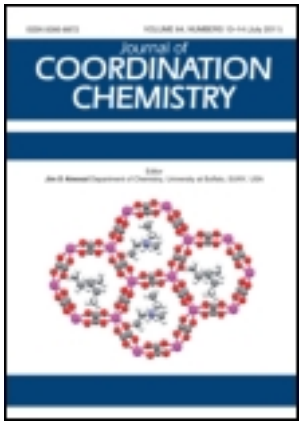

Journal of Coordination Chemistry
Publication details, including instructions for authors and subscription information:
http://www.tandfonline.com/loi/gcoo20

Preparation and structural characterization of oxovanadium(V) complexes with Schiff bases and their inhibition studies on Helicobacter pylori urease

Zhong-Lu You [a], Hui Sun [a], Bo-Wen Ding [a], Yu-Ping Ma [a], Mei Zhang [a] & Dong-Mei Xian [a]

[a] Department of Chemistry and Chemical Engineering, Liaoning Normal University, Huanghe Road 850#, Dalian 116029, P.R. China

Published online: 03 Oct 2011.

To cite this article: Zhong-Lu You, Hui Sun, Bo-Wen Ding, Yu-Ping Ma, Mei Zhang & Dong-Mei Xian (2011) Preparation and structural characterization of oxovanadium(V) complexes with Schiff bases and their inhibition studies on Helicobacter pylori urease, Journal of Coordination Chemistry, 64:20, 3510-3520, DOI: 10.1080/00958972.2011.625021

To link to this article: http://dx.doi.org/10.1080/00958972.2011.625021

Journal of Coordination Chemistry
Vol. 64, No. 20, 20 October 2011, 3510–3520

Preparation and structural characterization of oxovanadium(V) complexes with Schiff bases and their inhibition studies on *Helicobacter pylori* urease

ZHONG-LU YOU*, HUI SUN, BO-WEN DING, YU-PING MA, MEI ZHANG and DONG-MEI XIAN

Department of Chemistry and Chemical Engineering, Liaoning Normal University, Huanghe Road 850#, Dalian 116029, P.R. China

(*Received 29 June 2011; in final form 30 August 2011*)

A series of structurally similar dinuclear oxovanadium(V) complexes, $[VO_2L]_2$ ($L = L^1 =$ 2-[(2-methylaminoethylimino)methyl]phenolate (**1**); $L = L^2 =$ 2-[(2-ethylaminoethylimino) methyl]phenolate (**2**); $L = L^3 =$ 2-[(2-isopropylaminoethylimino)methyl]phenolate (**3**)), has been synthesized and characterized by physico-chemical methods and single-crystal X-ray diffraction. The V in each complex is octahedral, with three donors of L and one oxo defining the equatorial plane, and with two oxos occupying the axial positions. The complexes were tested for their urease inhibitory activities. The inhibition rate (%) of **1**, **2**, and **3** at 100 μmol L^{-1} on urease are 67 ± 1, 53.5 ± 0.9, and 44 ± 1. The relationship between structures of the complexes and the urease inhibitory activities indicates that shorter terminal groups of the complexes have stronger activities against urease. Molecular docking study of the complexes with the *Helicobacter pylori* urease was performed.

Keywords: Schiff base; Oxovanadium(V) complex; Crystal structure; Urease inhibition

1. Introduction

Schiff bases have received much attention in coordination and biological chemistry [1–3]. Vanadium complexes have been reported to have interesting biological activities such as normalizing high blood glucose levels and acting as models of haloperoxidases [4–6]. Ara and co-workers [7] reported that binuclear vanadium(IV) complexes possess interesting urease inhibitory activities. Our group indicated that mononuclear oxovanadium(V) complexes with Schiff bases also possess effective urease inhibitory activities [8]. To investigate the activities of binuclear vanadium complexes with Schiff bases, a series of binuclear oxovanadium(V) complexes, $[VO_2L]_2$ ($L = L^1 =$ 2-[(2-methylaminoethylimino)methyl]phenolate (**1**); $L = L^2 =$ 2-[(2-ethylaminoethylimino) methyl]phenolate (**2**); $L = L^3 =$ 2-[(2-isopropylaminoethylimino)methyl]phenolate (**3**); scheme 1), has been synthesized and structurally characterized. The urease inhibitory

*Corresponding author. Email: youzhonglu@yahoo.com.cn

ISSN 0095-8972 print/ISSN 1029-0389 online © 2011 Taylor & Francis
http://dx.doi.org/10.1080/00958972.2011.625021

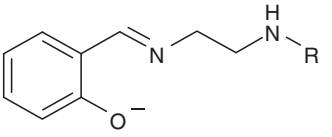

Scheme 1. The Schiff bases. R = methyl for L^1, ethyl for L^2, isopropyl for L^3.

activities of the complexes and the molecular docking analysis of the complexes with *Helicobacter pylori* urease were investigated.

2. Experimental

2.1. *General methods and materials*

Starting materials, reagents, and solvents were purchased from commercial suppliers in AR grade and used without purification. Elemental analyses were performed on a Perkin-Elmer 240C elemental analyzer. IR spectra were recorded on a Jasco FT/IR-4000 spectrometer as KBr pellets from 4000 to 200 cm^{-1}. ^1H NMR spectra were recorded on a Bruker AVANCE 400 MHz spectrometer with tetramethylsilane as the internal reference. Molar conductance was measured with a Shanghai DDS-11A conductometer. X-ray diffraction was carried out on a Bruker SMART 1000 CCD diffractometer. The Schiff bases HL^1, HL^2, and HL^3 were prepared according to the literature method [9].

2.2. *Synthesis of the complexes*

$[VO_2L^1]_2$ (**1**): A methanolic solution (30 mL) of $VO(acac)_2$ (0.27 g, 1.0 mmol) was added to a methanolic solution (20 mL) of HL^1 (0.18 g, 1.0 mmol) with stirring. The mixture was stirred at room temperature for 30 min to give a brown solution. The resulting solution was allowed to stand in air for a week until 5 mL of the solvent remained. Brown block-shaped crystals of **1** suitable for X-ray single-crystal diffraction formed at the bottom of the vessel. The crystals were isolated, washed three times with cold methanol, and dried in air. Yield 62%. IR data (cm^{-1}): 3246 (sh, m), 1649 (s), 1598 (m), 1549 (m), 1471 (m), 1451 (s), 1390 (w), 1333 (w), 1327 (s), 1202 (w), 1147 (w), 1122 (w), 1087 (w), 1031 (w), 1012 (w), 934 (s), 845 (s), 798 (w), 754 (m), 623 (m), 533 (w), 461 (w), 445 (w), 399 (w), 373 (w), 342 (w), 303 (w). Anal. Calcd for $C_{20}H_{26}N_4O_6V_2$: C, 46.2; H, 5.0; N, 10.8. Found (%): C, 46.5; H, 5.2; N, 10.6.

$[VO_2L^2]_2$ (**2**): Complex **2** was synthesized by the same method as described for **1**, with HL^1 replaced by HL^2 (0.19 g, 1.0 mmol). Brown block-shaped single crystals of **2** were isolated after a week, washed three times with cold MeOH, and dried in air. Yield 53%. IR data (cm^{-1}): 3221 (sh, m), 1634 (s), 1601 (m), 1549 (m), 1472 (m), 1448 (s), 1394 (w), 1338 (w), 1292 (s), 1207 (w), 1151 (w), 1127 (w), 1088 (w), 1064 (m), 1020 (m), 929 (s), 846 (s), 805 (w), 760 (m), 623 (m), 553 (w), 465 (w), 446 (w), 393 (w), 378 (w) 350 (w),

Table 1. Crystallographic and experimental data for **1–3**.

Complex	**1**	**2**	**3**
Empirical formula	$C_{20}H_{26}N_4O_6V_2$	$C_{22}H_{30}N_4O_6V_2$	$C_{24}H_{34}N_4O_6V_2$
Formula weight	520.3	548.4	576.4
Crystal system	Monoclinic	Triclinic	Triclinic
Space group	$P2_1/c$	$P\bar{1}$	$P\bar{1}$
Unit cell dimensions (Å, °)			
a	6.678(2)	7.685(1)	9.377(1)
b	11.955(3)	8.848(2)	9.510(1)
c	13.830(3)	10.634(2)	15.489(2)
α	90	66.098(2)	74.535(2)
β	92.161(3)	72.935(2)	76.866(2)
γ	90	66.981(2)	77.901(1)
Volume (Å^3), Z	1103.3(5), 2	600.6(2), 1	1279.9(3), 2
Calculated density (g cm^{-3})	1.566	1.516	1.496
Absorption coefficient (Mo-Kα) (mm^{-1})	0.892	0.823	0.777
F(000)	536	284	600
Independent reflections	2364	2403	5413
Observed reflections ($I \geq 2\sigma(I)$)	1972	2222	3757
Min. and max. transmission	0.795 and 0.801	0.790 and 0.808	0.842 and 0.848
Parameters	150	158	335
Restraints	1	1	2
Goodness-of-fit on F^2	1.042	1.063	1.056
R_1, wR_2 [$I \geq 2\sigma(I)$][a]	0.0539, 0.1414	0.0315, 0.0830	0.0522, 0.1295
R_1, wR_2 (all data)[a]	0.0633, 0.1477	0.0343, 0.0847	0.0782, 0.1443

[a] $R_1 = F_o - F_c/F_o$, $wR_2 = [\Sigma w(F_o^2 - F_c^2)/\Sigma w(F_o^2)^2]^{1/2}$.

302 (w). Anal. Calcd for $C_{22}H_{30}N_4O_6V_2$: C, 48.2; H, 5.5; N, 10.2. Found (%): C, 48.0; H, 5.6; N, 10.4.

$[VO_2L^3]_2$ (**3**): Complex **3** was synthesized by the same method as described for **1**, with HL^1 replaced by HL^3 (0.21 g, 1.0 mmol). The brown block-shaped single crystals of **3** were isolated after a week, washed three times with cold MeOH, and dried in air. Yield 71%. IR data (cm^{-1}): 3221 (sh, m), 1644 (s), 1597 (m), 1549 (m), 1471 (m), 1448 (s), 1395 (w), 1325 (w), 1294 (s), 1204 (w), 1150 (w), 1125 (w), 1080 (w), 1028 (m), 931 (s), 855 (s), 768 (w), 621 (m), 551 (w), 459 (w), 426 (w), 377 (w), 345 (w). Anal. Calcd for $C_{24}H_{34}N_4O_6V_2$: C, 50.0; H, 5.9; N, 9.7. Found (%): C, 49.7; H, 6.0; N, 9.8.

2.3. *X-ray crystallography*

Diffraction intensities for the complexes were collected at 298(2) K using a Bruker SMART 1000 CCD area-detector diffractometer with Mo-Kα radiation ($\lambda = 0.71073$ Å). The collected data were reduced with SAINT [10], and multi-scan absorption correction was performed using SADABS [11]. The structures were solved by direct methods. The complexes were refined against F^2 by full-matrix least-squares using the SHELXTL package [12]. All non-hydrogen atoms were refined anisotropically. The amino hydrogen atoms in the complexes are located from difference Fourier maps and refined isotropically, with N–H distances restrained to 0.90(1) Å. The remaining hydrogen atoms were placed in calculated positions and constrained to ride on their parent atoms. The crystallographic data for the complexes are summarized in table 1. Selected bond lengths and angles are given in table 2.

Table 2. Selected bond lengths (Å) and angles (°) for **1–3**.

1			
V1–O1	1.920(2)	V1–O2	1.611(2)
V1–O3	1.669(2)	V1–N1	2.153(3)
V1–N2	2.143(3)	V1–O3^{i}	2.312(2)
O2–V1–O3	105.7(1)	O2–V1–O1	102.3(1)
O3–V1–O1	98.7(1)	O2–V1–N2	94.0(1)
O3–V1–N2	92.8(1)	O1–V1–N2	156.6(1)
O2–V1–N1	95.4(1)	O3–V1–N1	157.1(1)
O1–V1–N1	84.9(1)	N2–V1–N1	76.8(1)
O2–V1–O3^{i}	171.5(1)	O3–V1–O3^{i}	78.7(1)
O1–V1–O3^{i}	84.0(1)	N2–V1–O3^{i}	78.4(1)
N1–V1–O3^{i}	79.2(1)		
2			
V1–O1	1.907(1)	V1–O2	1.612(2)
V1–O3	2.385(1)	V1–N1	2.158(2)
V1–N2	2.149(2)	V1–O3^{ii}	1.665(1)
O2–V1–O3	107.8(1)	O2–V1–O1	102.6(1)
O3^{ii}–V1–O1	98.7(1)	O2–V1–N2	92.5(1)
O3^{ii}–V1–N2	92.0(1)	O1–V1–N2	157.8(1)
O2–V1–N1	97.3(1)	O3^{ii}–V1–N1	153.0(1)
O1–V1–N1	84.9(1)	N2–V1–N1	77.0(1)
O2–V1–O3	169.8(1)	O3^{ii}–V1–O3	78.0(1)
O1–V1–O3	84.4(1)	N2–V1–O3	78.8(1)
N1–V1–O3	75.7(1)		
3			
V1–O1	1.913(2)	V1–O2	1.666(2)
V1–O3	1.609(2)	V1–N1	2.154(3)
V1–N2	2.171(3)	V1–O2^{iii}	2.410(3)
O3–V1–O2	108.9(1)	O3–V1–O1	100.1(1)
O2–V1–O1	99.1(1)	O3–V1–N1	95.6(1)
O2–V1–N1	154.2(1)	O1–V1–N1	84.2(1)
O3–V1–N2	95.5(1)	O2–V1–N2	92.1(1)
O1–V1–N2	156.6(1)	N1–V1–N2	77.1(1)
O3–V1–O2^{iii}	170.2(1)	O2–V1–O2^{iii}	78.5(1)
O1–V1–O2^{iii}	84.6(1)	N1–V1–O2^{iii}	76.3(1)
N2–V1–O2^{iii}	77.6(1)		

Symmetry codes: $^{i}2-x, 2-y, 1-z$; $^{ii}1-x, -y, 1-z$; $^{iii}1-x, 1-y, 1-z$.

2.4. *Urease inhibitory activity assay*

Helicobacter pylori (ATCC 43504; American Type Culture Collection, Manassas, VA) was grown in brucella broth supplemented with 10% heat-inactivated horse serum for 24 h at 37°C under microaerobic conditions (5% O_2, 10% CO_2, and 85% N_2). The method of preparation of *H. pylori* urease by Mao *et al.* [13] was followed. Briefly, broth cultures (50 mL, 2.0×10^8 CFU mL^{-1}) were centrifuged (5000 g, 4°C) to collect the bacteria, and after washing twice with phosphate-buffered saline (pH 7.4), the *H. pylori* precipitate was stored at −80°C. While the *H. pylori* was returned to room temperature, and mixed with 3 mL of distilled water and protease inhibitors, sonication was performed for 60 s. Following centrifugation (15,000 g, 4°C), the supernatant was desalted through SephadexG–25 column (PD–10 columns, Amersham-Pharmacia Biotech, Uppsala, Sweden). The resultant crude urease solution was added to an equal volume of glycerol and stored at 4°C until use in the experiment. The mixture,

containing 25 μL (4U) of *H. pylori* urease and 25 μL of the test compound, was pre-incubated for 3 h at room temperature in a 96-well assay plate. Urease activity was determined for three parallel times by measuring ammonia production using the indophenol method as described by Weatherburn [14].

2.5. *Molecular docking study*

Molecular docking of the complexes into the 3-D X-ray structures of *H. pylori* urease structure (entry 1E9Y in the Protein Data Bank) was carried out by using the AutoDock 4.2 software as implemented through the graphical user interface AutoDockTools (ADT 1.5.4). The graphical user interface AutoDockTools was employed to setup the enzymes: all hydrogen atoms were added, Gasteiger charges were calculated, and non-polar hydrogen atoms were merged to carbon atoms. The Ni initial parameters are set as $r = 1.170$ Å, $q = +2.0$, and van der Waals well depth of $0.100\,\text{kcalmol}^{-1}$ [15]. The molecules of **1** and **2**, and the V1 molecule of **3** were transferred to pdb files with the program ChemBio3D. The pdb files were further transferred to pdbqt files with AutoDockTools.

AutoDockTools was used to generate the docking input files. In all docking, a grid box with a size of $70 \times 60 \times 60$ points in x, y, and z directions was built, the maps were centered on the original ligand molecule in the catalytic site of the protein. A grid spacing of 0.375 Å and a distances-dependent function of the dielectric constant were used for the calculation of the energy map. 100 runs were generated by using Lamarckian genetic algorithm searches. Default settings were used with an initial population of 50 randomly placed individuals, a maximum number of 2.5×10^6 energy evaluations, and a maximum number of 2.7×10^4 generations. A mutation rate of 0.02 and a crossover rate of 0.8 were chosen. The results of the most favorable free energy of binding were selected as the resultant complex structures.

3. Results and discussion

3.1. *Chemistry*

The Schiff bases were synthesized by the reaction of salicylaldehyde with *N*-alkylethane-1,2-diamine in absolute methanol, with high yields and purity. The complexes were synthesized by reaction of the Schiff bases with $VO(acac)_2$ in a molar ratio of 1 : 1 in methanol. Single crystals were obtained by slow evaporation of methanolic solutions of the complexes. All complexes are stable in air at room temperature. Molar conductivities of the complexes in MeOH at $10^{-3}\,\text{molL}^{-1}$ are $24\,\Omega^{-1}\,\text{cm}^2\,\text{mol}^{-1}$ for **1**, $22\,\Omega^{-1}\,\text{cm}^2\,\text{mol}^{-1}$ for **2**, and $16\,\Omega^{-1}\,\text{cm}^2\,\text{mol}^{-1}$ for **3**, and at concentration of $10^{-2}\,\text{molL}^{-1}$ are $172\,\Omega^{-1}\,\text{cm}^2\,\text{mol}^{-1}$ for **1**, $160\,\Omega^{-1}\,\text{cm}^2\,\text{mol}^{-1}$ for **2**, and $135\,\Omega^{-1}\,\text{cm}^2\,\text{mol}^{-1}$ for **3**, indicating the non-electrolytic nature of the complexes in solution [16]. When compared with the mononuclear oxovanadium(V) complexes derived from similar Schiff bases [8, 17, 18], the secondary amine groups are essential for the dimeric structures.

3.2. *Structure description of the complexes*

The molecular structures of **1**, **2**, and **3** are shown in figures 1, 2, and 3, respectively. X-ray crystallography reveals that the complexes are similar centrosymmetric dimeric oxovanadium(V) compounds. The difference among the complexes is different Schiff-base ligands. Complex **1** is isostructural with that (**1′**) reported by Mokry and Carrano [19], but with different space groups. The obvious difference between the structures of **1** and **1′** is the lengths of the apical bonds (2.312(2) Å for **1** and 2.437(2) Å for **1′**), following with the shorter V···V distance in **1** (3.106(1) Å) than that in **1′** (3.225(1) Å).

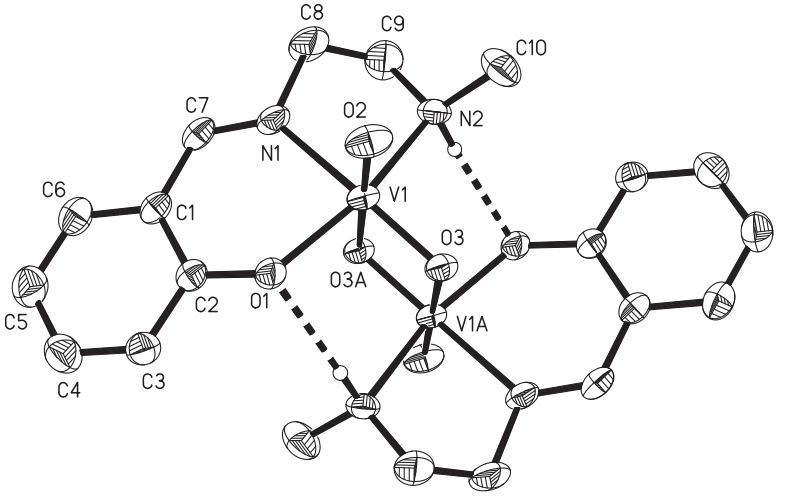

Figure 1. Perspective view of the molecular structure of **1** with the atom labeling scheme. The thermal ellipsoids are drawn at the 30% probability level.

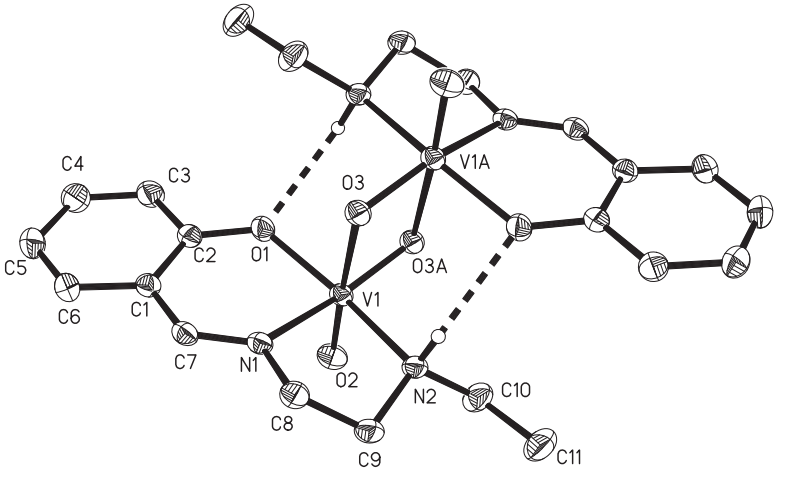

Figure 2. Perspective view of the molecular structure of **2** with the atom labeling scheme. The thermal ellipsoids are drawn at the 30% probability level.

The slight difference of the apical bonds leads to the distinct molecular packing modes of the compounds (figure 4). In the molecular packing of **1**, the molecules are stacked with no obvious short contacts, while in **2**, the molecules are linked *via* non-typical intermolecular C–H···O hydrogen bonds, leading to formation of 2-D sheets parallel to the *ab* plane. The V···V distances are 3.179(1) Å for **2**, 3.195(1) and 3.191(1) Å for **3**. Each V in the complexes is six-coordinate through three bonds to oxo groups and through three bonds to the tridentate Schiff-base ligand, forming an octahedral geometry. The distances between V1 and O3 in **1** and **2**, V1 and O2 and V2 and O5 in **3** are in the range 1.658(2)–1.669(2) Å, indicating they are typical V=O bonds. O3 in **1** and **2**, O2 and O5 atoms in **3** are bridging groups. The coordinate bond lengths in the complexes are comparable to each other. Distortion of the octahedral coordination can be observed by the coordinate bond angles, ranging from 76.8(1) to 105.7(1)° (**1**), 77.0(1) to 107.8(1)° (**2**), and 76.0(1) to 108.9(1)° for the perpendicular angles, and from 156.6(1) to 171.5(1)° (**1**), 153.0(1) to 169.8(1)° (**2**), and 153.4(1) to 170.4(1)° (**3**) for the

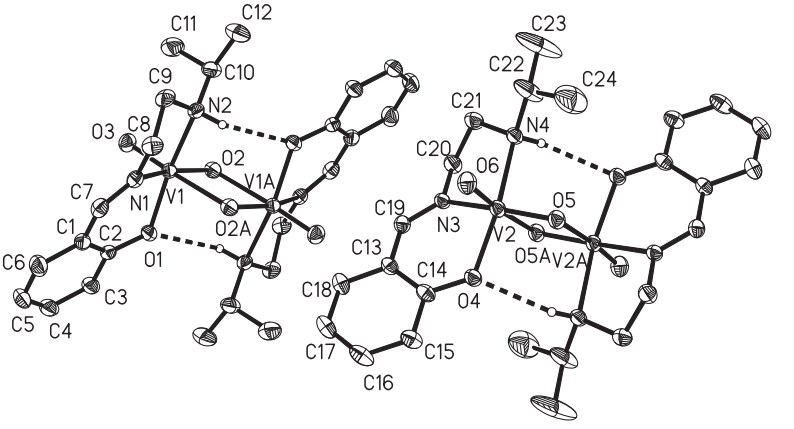

Figure 3. Perspective view of the molecular structure of **3** with the atom labeling scheme. The thermal ellipsoids are drawn at the 30% probability level.

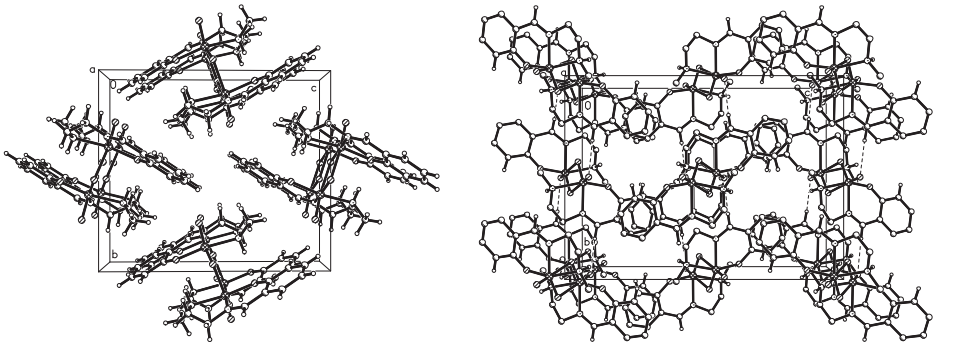

Figure 4. The molecular packing of **1** (left) and **1′** (right) viewed along the *a*-axis. Intermolecular C–H···O hydrogen bonds are drawn as dashed lines.

Table 3. Inhibition of urease by the tested materials.

Tested materials	Inhibition rate[a] (%)	IC_{50} ($\mu mol\,L^{-1}$)
1	67.3 ± 1.3	71.2 ± 3.5
2	53.5 ± 0.9	86.7 ± 2.1
3	44.4 ± 1.2	–
HL^1	12.7 ± 1.5	–
HL^2	8.3 ± 0.9	–
HL^3	6.5 ± 1.2	–
Vanadyl sulfate	22.3 ± 2.7	207.1 ± 3.1
AHA	90.2 ± 3.7	43.1 ± 2.7

[a]The concentration of the tested material is $100\,\mu mol\,L^{-1}$.

diagonal angles. In each complex, there are two intramolecular N–H···O hydrogen bonds in the dimeric molecule.

3.3. *IR spectra*

Weak and broad absorptions centered at $3425\,cm^{-1}$ indicate the presence of phenol groups in the Schiff bases and are absent in the complexes. Strong absorption bands at $1615–1618\,cm^{-1}$ in spectra of the Schiff bases assigned to the azomethine ν(C=N) [20] shift to higher wavenumbers in the complexes, $1634–1649\,cm^{-1}$, attributed to coordination of imine nitrogen to vanadium. The middle absorption bands of Ar–O in the Schiff bases at $1223–1280\,cm^{-1}$ [21] are located at lower frequencies for the complexes, namely $1202\,cm^{-1}$ for **1**, $1207\,cm^{-1}$ for **2**, and $1204\,cm^{-1}$ for **3**. The strong absorptions at $930\,cm^{-1}$ and $850\,cm^{-1}$ are assigned to V=O vibrations.

The close resemblance of the shape and the positions of the bands suggest similar coordination modes for the complexes, in accord with structural features.

3.4. *Pharmacology*

The results of urease inhibition are summarized in table 3. Acetohydroxamic acid (AHA) was used as a reference. The complexes exhibited moderate to effective inhibition. The complexes inhibit urease in the order **1** > **2** > **3**. The IC_{50} values ($71 \pm 3\,\mu mol\,L^{-1}$ for **1** and $87 \pm 2\,\mu mol\,L^{-1}$ for **2**) were determined since they have effective urease inhibitory activities. The results indicate that the inhibitory activities of the complexes are much better than vanadyl sulfate with an IC_{50} value of $207 \pm 3\,\mu mol\,L^{-1}$. However, when compared with AHA, the activities of the complexes are relatively weak. Considering that the difference of the structures is only the terminal alkyl of the Schiff base, namely methyl for **1**, ethyl for **2**, and isopropyl for **3**, it is easy to conclude that the shorter the terminal groups of the Schiff base, the stronger the urease inhibitory activities of the oxovanadium(V) complexes. The results are in accord with that reported previously [22].

3.5. *Molecular docking study*

Molecular docking was performed to investigate the binding effects between the complexes and the active sites of the *H. pylori* urease. In the X-ray structure available

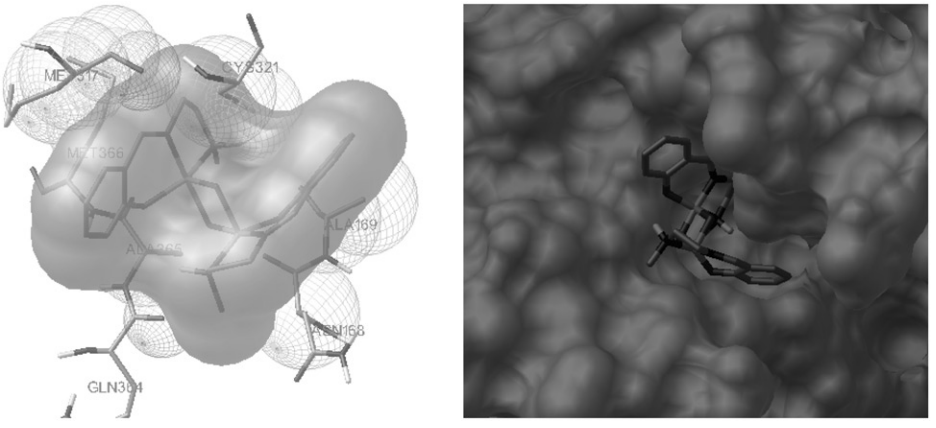

Figure 5. Binding mode of **1** with *H. pylori* urease. Left: only the interacting residues are displayed. The interactions are shown as dashed spheres. Right: the enzyme is shown as surface. The complex is shown as sticks.

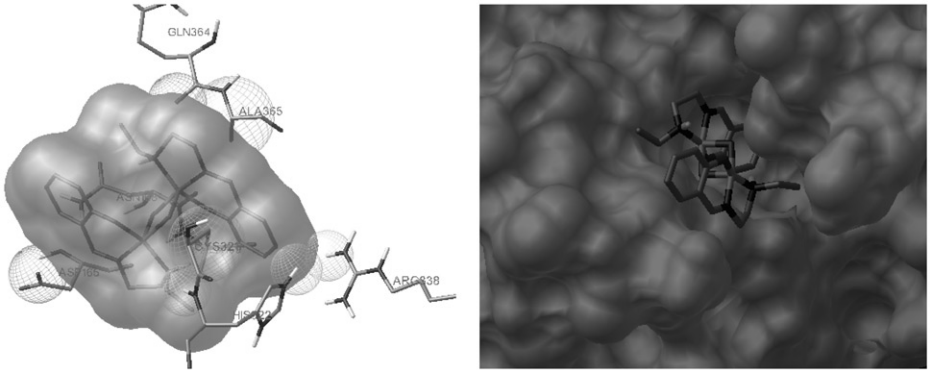

Figure 6. Binding mode of **2** with *H. pylori* urease. Left: only the interacting residues are displayed. The interactions are shown as dashed spheres. Right: the enzyme is shown as surface. The complex is shown as sticks.

for the native *H. pylori* urease, two nickels were coordinated by *His*136, *His*138, *Kcx*219, *His*248, *His*274, *Asp*362, and water, while in the AHA-inhibited urease, water molecules were replaced by AHA [23]. To understand the inhibitory activity of the complexes, molecular docking of the complexes into the AHA-binding site of the urease was performed on the binding model based on the *H. pylori* urease complex structure (1E9Y.pdb). The binding models of the complexes and the urease are depicted in figures 5–7, revealing that the complex molecules fit in the active pocket of the urease. The binding energy of the complexes with urease are $-6.75\,\mathrm{kcalmol^{-1}}$ for **1**, $-6.32\,\mathrm{kcalmol^{-1}}$ for **2**, and $-5.86\,\mathrm{kcalmol^{-1}}$ for **3**, lower than that of the AHA ($-5.01\,\mathrm{kcalmol^{-1}}$). The results of the molecular docking study agree with the inhibitory order of **1** > **2** > **3**, and could explain the activity of the complexes against *H. pylori* urease.

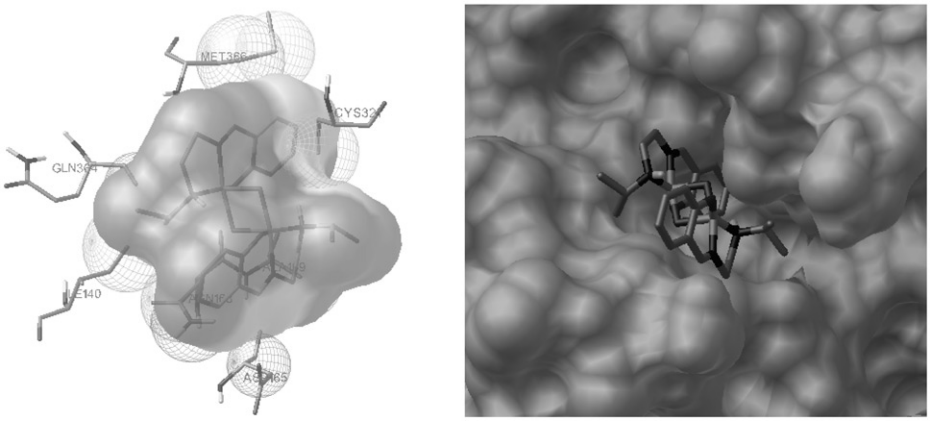

Figure 7. Binding mode of **3** with *H. pylori* urease. Left: only the interacting residues are displayed. The interactions are shown as dashed spheres. Right: the enzyme is shown as surface. The complex is shown as sticks.

4. Conclusion

This study reports the synthesis and structures of three dimeric oxovanadium(V) complexes with similar Schiff bases. The complexes show from moderate to effective inhibitory activities against *H. pylori* urease. The structure–activity relationship indicates that shorter terminal groups of the Schiff-base ligands have stronger urease inhibitory activities of the oxovanadium(V) complexes. The complexes may be used in the treatment of infections caused by urease producing bacteria.

Supplementary material

CCDC 830072 (**1**), 830073 (**2**), and 830074 (**3**) contain the supplementary crystallographic data for this article. These data can be obtained free of charge *via* http://www.ccdc.cam.ac.uk/conts/retrieving.html, or from the Cambridge Crystallographic Data Centre, 12 Union Road, Cambridge CB2 1EZ, UK; Fax: (+44) 1223-336-033; or E-mail: deposit@ccdc.cam.ac.uk.

Acknowledgments

This work was financially supported by the National Science Foundation of China (Project No. 20901036).

References

[1] L. Shi, W.-J. Mao, Y. Yang, H.-L. Zhu. *J. Coord. Chem.*, **62**, 3471 (2009).
[2] K. Cheng, Q.-Z. Zheng, Y. Qian, L. Shi, J. Zhao, H.-L. Zhu. *Bioorg. Med. Chem.*, **17**, 7861 (2009).

[3] Z.-L. You, D.-H. Shi, C. Xu, Q. Zhang, H.-L. Zhu. *Eur. J. Med. Chem.*, **43**, 862 (2008).
[4] G.R. Willsky, A.B. Goldfine, P.J. Kostyniak, J.H. McNeill, L.Q. Yang, H.R. Khan, D.C. Crans. *J. Inorg. Biochem.*, **85**, 33 (2001).
[5] C. Orvig, P. Caravan, L. Gelmini, N. Glover, F.G. Herring, H. Li, J.H. McNeill, S.J. Rettig, I.A. Setyawati. *J. Am. Chem. Soc.*, **117**, 12759 (1995).
[6] A. Messerschmidt, L. Prade, R. Wever. *Biol. Chem.*, **378**, 309 (1997).
[7] R. Ara, U. Ashiq, M. Mahroof-Tahir, Z.T. Maqsood, K.M. Khan, M.A. Lodhi, M.I. Choudhary. *Chem. Biodivers.*, **4**, 58 (2007).
[8] Z.-L. You, Y.-M. Cui, Y.-P. Ma, C. Wang, X.-S. Zhou, K. Li. *Inorg. Chem. Commun.*, **14**, 636 (2011).
[9] Z.-L. You, H.-L. Zhu. *Z. Anorg. Allg. Chem.*, **632**, 140 (2006).
[10] Bruker. *SMART* (Version 5.628) and *SAINT* (Version 6.02), Bruker AXS Inc., Madison, Wisconsin, USA (1998).
[11] G.M. Sheldrick. *SADABS Program for Empirical Absorption Correction of Area Detector*, University of Göttingen, Germany (1996).
[12] G.M. Sheldrick. *Acta Crystallogr.*, **A64**, 112 (2008).
[13] W.-J. Mao, P.-C. Lv, L. Shi, H.-Q. Li, H.-L. Zhu. *Bioorg. Med. Chem.*, **17**, 7531 (2009).
[14] M.W. Weatherburn. *Anal. Chem.*, **39**, 971 (1967).
[15] B. Krajewska, W. Zaborska. *Bioorg. Chem.*, **35**, 355 (2007).
[16] W.J. Geary. *Coord. Chem. Rev.*, **7**, 81 (1971).
[17] M.-J. Xie, Y.-S. Ping, L.-D. Zheng, J.-Z. Hui, C. Peng. *Acta Crystallogr.*, **E60** (2004).
[18] J. Hartung, S. Drees, M. Greb, P. Schmidt, I. Svoboda, H. Fuess, A. Murso, D. Stalke. *Eur. J. Org. Chem.*, **13**, 2388 (2003).
[19] L.M. Mokry, C.J. Carrano. *Inorg. Chem.*, **32**, 6119 (1993).
[20] J.E. Kovacic. *Spectrochim. Acta*, **A23**, 183 (1963).
[21] G.C. Percy, D.A. Thornton. *J. Inorg. Nucl. Chem.*, **34**, 3357 (1972).
[22] Z.-L. You, Y.-M. Cui, Y.-P. Ma, C. Wang, X.-S. Zhou, K. Li. *Inorg. Chem. Commun.*, **14**, 636 (2011).
[23] Z.-P. Xiao, T.-W. Ma, W.-C. Fu, X.-C. Peng, A.-H. Zhang, H.-L. Zhu. *Eur. J. Med. Chem.*, **45**, 5064 (2010).